Han *et al. J Mater Inf* 2023;Volume:Number
DOI: 10.20517/jmi.xxx.xx

Journal of Materials Informatics

Open Access

Supplementary Material:

Regulating the Electrocatalytic Performance for Nitrogen Reduction Reaction by Tuning the N Contents in $Fe_3@N_xC_{20-x}$ (x = 0~4): A DFT Exploration

How to Use This Template

This template shows the manuscript structure that can be used in supplementary material. Please note that each part has a corresponding style, which authors should follow. Please note that the fonts in gray show writing requirements. For any questions, you may contact the editorial office.

Supplementary Table 1. The corrected values of gas molecules (in eV).

Gas	
N_2	−0.35
H_2	−0.05
NH_3	0.42

Supplementary Table 2. The corrected values of intermediates on $Fe_3@C_{20}$ and $Fe_3@N_4C_{16}$ (in eV).

Reaction routes		Intermediates						
$Fe_3@C_{20}$	Consecutive	*NN	*NNH	*NNH_2	*N	*NH	*NH_2	*NH_3
		0.13	0.44	0.65	0.08	0.34	0.67	0.95
	Enzymatic	*NN	*NNH	*NHNH	*NH_2NH	*NH_2NH_2	*NH_2	*NH_3
		0.13	0.44	0.74	1.08	1.42	0.67	0.95
	Distal	*NN	*NNH	*NNH_2	*N	*NH	*NH_2	*NH_3
		0.10	0.43	0.73	0.07	0.34	0.66	0.95
	Alternative	*NN	*NNH	*NHNH	*NH_2NH	*NH_2NH_2	*NH_2	*NH_3
		0.10	0.43	0.78	0.97	1.42	0.66	0.96
$Fe_3@N_4C_{16}$	Consecutive	*NN	*NNH	*NNH_2	*N	*NH	*NH_2	*NH_3
		0.08	0.44	0.65	0.08	0.34	0.67	0.95
	Enzymatic	*NN	*NNH	*NHNH	*NH_2NH	*NH_2NH_2	*NH_2	*NH_3
		0.08	0.44	0.74	1.08	1.42	0.67	0.95

Supplementary Table 3. Formation energies (E_f, in eV) of $Fe_3@N_xC_{20-x}$ with Fe_2-bonded C replaced by N (*x* is the number of N atoms).

x	1	2-I	2-II	2-III	3	4
structure	Supplementary Figure 4A	Supplementary Figure 4B	Supplementary Figure 4C	Supplementary Figure 4D	Supplementary Figure 4E	Supplementary Figure 4F
E_f	−0.20	−0.22	−0.50	−0.35	−0.33	−0.65

Supplementary Table 4. Lattice constants (*a* and *b*, in Å) of $Fe_3@N_xC_{20-x}$, nitrogen adsorption energies on Fe_2 sites and Fe_1 sites (E_{ads}, in eV).

	a	*b*	Fe_2 site		Fe_1 site	
			E_{ads} (end-on)	E_{ads} (side-on)	E_{ads} (end-on)	E_{ads} (side-on)
$Fe_3@C_{20}$	11.14	7.95	−0.52	−0.57	−0.41	−0.10
$Fe_3@N_1C_{19}$	11.08	7.90	−0.55	−0.62	−0.43	−0.11
$Fe_3@N_2C_{18}$-I	11.00	7.91	−0.59	−0.55	−0.39	−0.06
$Fe_3@N_2C_{18}$-II	11.02	7.73	−0.50	−0.48	−0.47	−0.08
$Fe_3@N_2C_{18}$-III	11.04	7.66	−0.59	−0.52	−0.43	−0.17
$Fe_3@N_3C_{17}$	10.95	7.85	−0.54	−0.52	−0.58	−0.08
$Fe_3@N_4C_{16}$	10.87	7.74	−0.32	−0.20	−0.44	0.15

Supplementary Table 5. The free energy change (ΔG, in eV) of the step *NN→*NNH (in eV).

	end-on	side-on
$Fe_3@C_{20}$	0.59	0.64
$Fe_3@N_1C_{19}$	1.14	0.74
$Fe_3@N_2C_{18}$-I	1.09	0.61
$Fe_3@N_2C_{18}$-II	1.07	0.73
$Fe_3@N_2C_{18}$-III	0.65	0.71
$Fe_3@N_3C_{17}$	1.08	0.67
$Fe_3@N_4C_{16}$	/	0.45

Supplementary Table 6. The Fe−Fe bond lengths (d_{Fe-Fe}) and *d*-band centers and *p*-band centers of the Fe_2-bonded C/N for $Fe_3@N_xC_{20-x}$ (x = 0~4).

	d_{Fe-Fe} (Å)	*d*-band centers	*p*-band centers of Fe_2-bonded C and N atoms
$Fe_3@C_{20}$	2.22	−0.92	−3.51
$Fe_3@N_1C_{19}$	2.22	−0.92	−3.57
$Fe_3@N_2C_{18}$-I	2.23	−0.91	−4.43
$Fe_3@N_2C_{18}$-II	2.22	−1.05	−4.02
$Fe_3@N_2C_{18}$-III	2.24	−1.05	−3.96
$Fe_3@N_3C_{17}$	2.23	−1.00	−4.81
$Fe_3@N_4C_{16}$	2.16	−0.98	−3.89

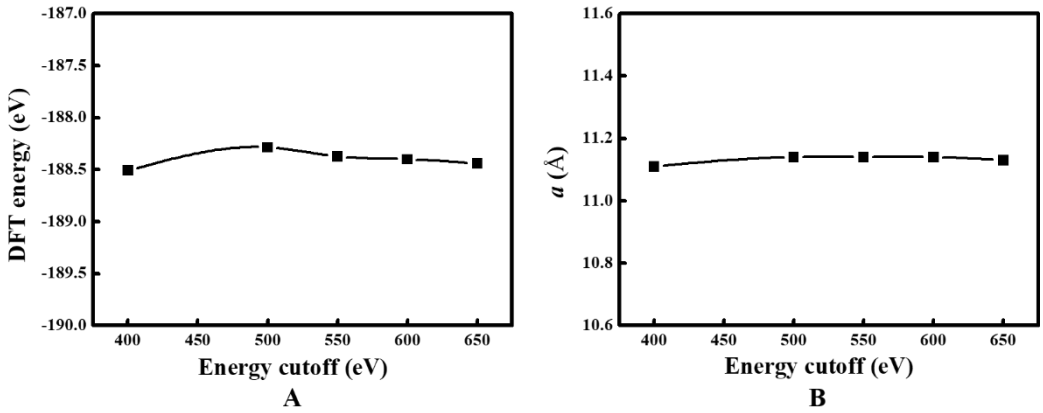

Supplementary Figure 1. Evaluation of energy cutoff for optimizing $Fe_3@C_{20}$: the variation of the total DFT energy (A) and the lattice constant *a* (B) against energy cutoff.

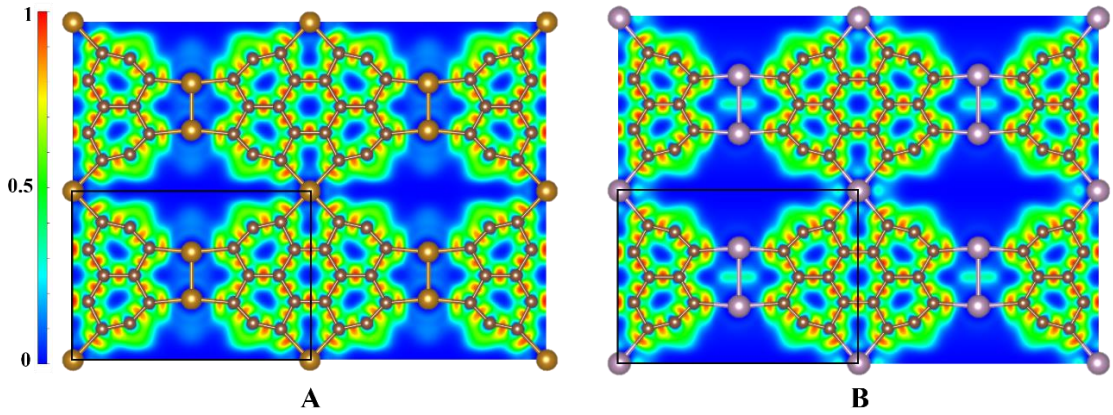

Supplementary Figure 2. The ELF plot of (110) section of $Fe_3@C_{20}$(A) and $Mo_3@C_{20}$(B) monolayer, with the unit cells marked by black lines.

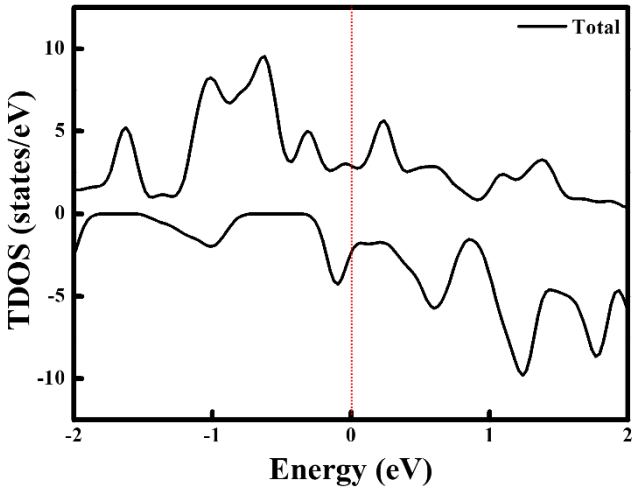

Supplementary Figure 3. The TDOS of 2D $Mo_3@C_{20}$ monolayer with the Fermi energy level indicated by the red dashed line.

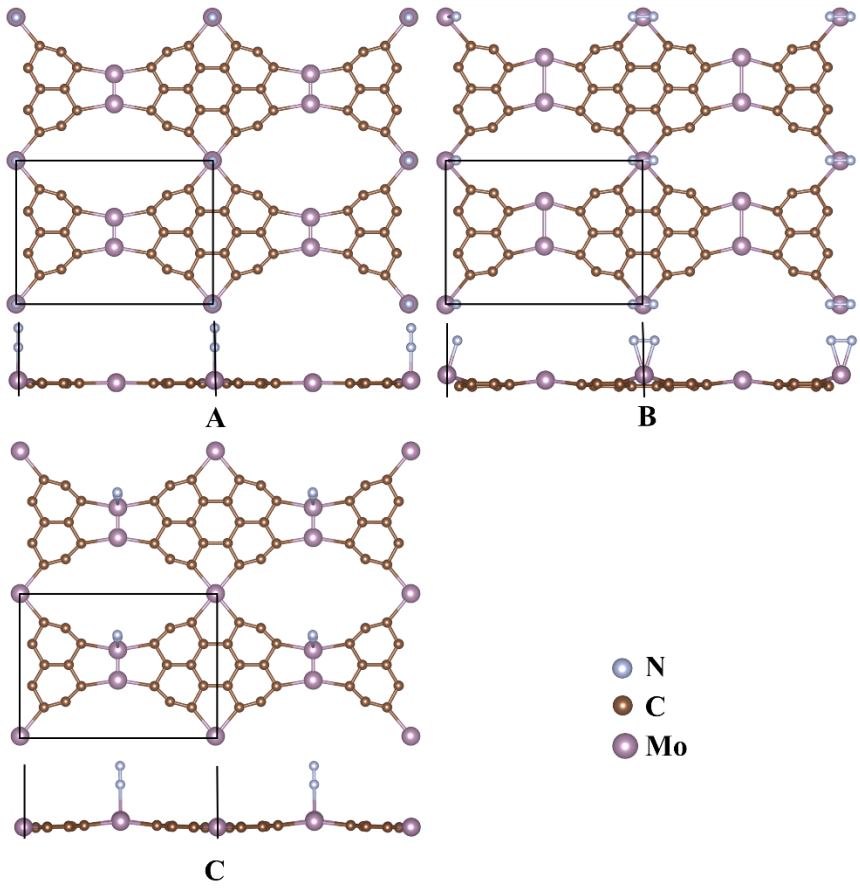

Supplementary Figure 4. Different adsorption structures of N_2 on $Mo_3@C_{20}$: (A) end-on and (B) side-on configuration at Mo_1 site, and (C) end-on and configuration at Mo_2 site, with the unit cells marked by black lines.

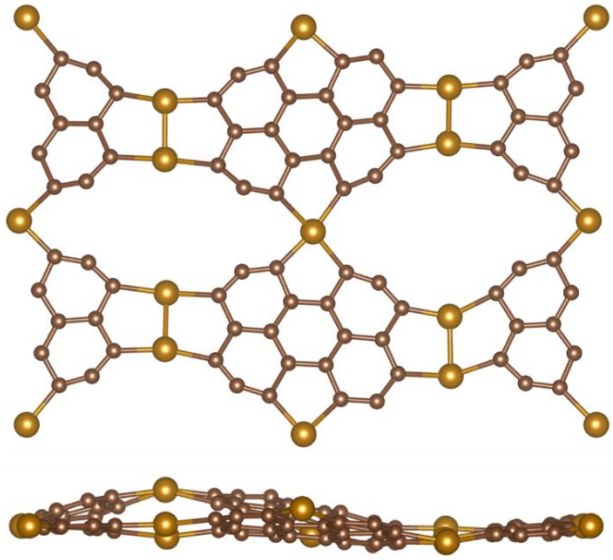

Supplementary Figure 5. The final structure of $Fe_3@C_{20}$ after 5-ps' FPMD simulations at 300 K.

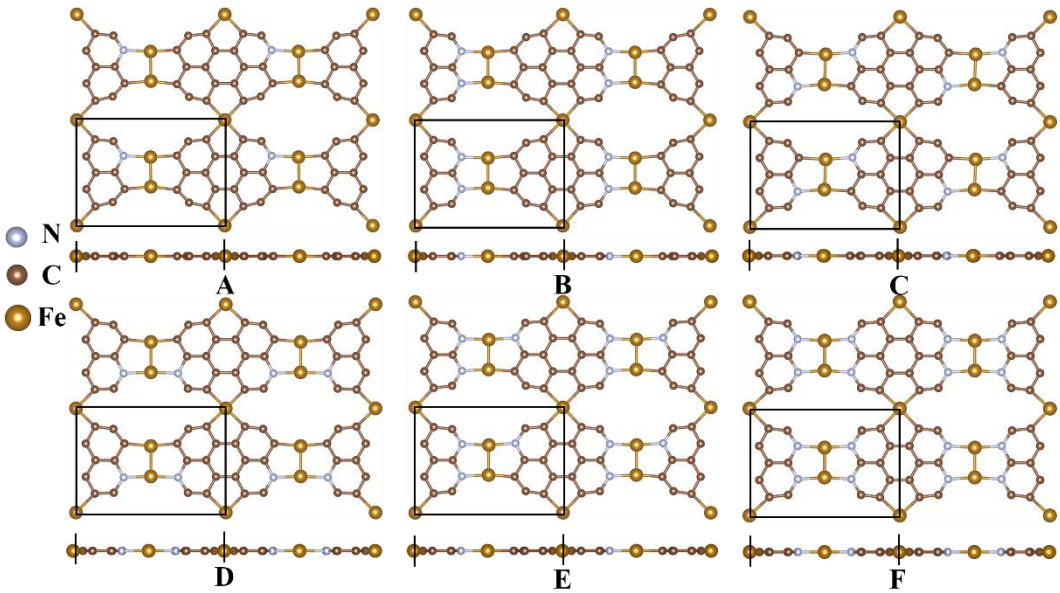

Supplementary Figure 6. The top and side views of $Fe_3@N_1C_{19}$ (A), $Fe_3@N_2C_{18}$-I (B), $Fe_3@N_2C_{18}$-II (C), $Fe_3@N_2C_{18}$-III (D), $Fe_3@N_3C_{17}$ (E), and $Fe_3@N_4C_{16}$ (F), with the unit cells marked by black lines.

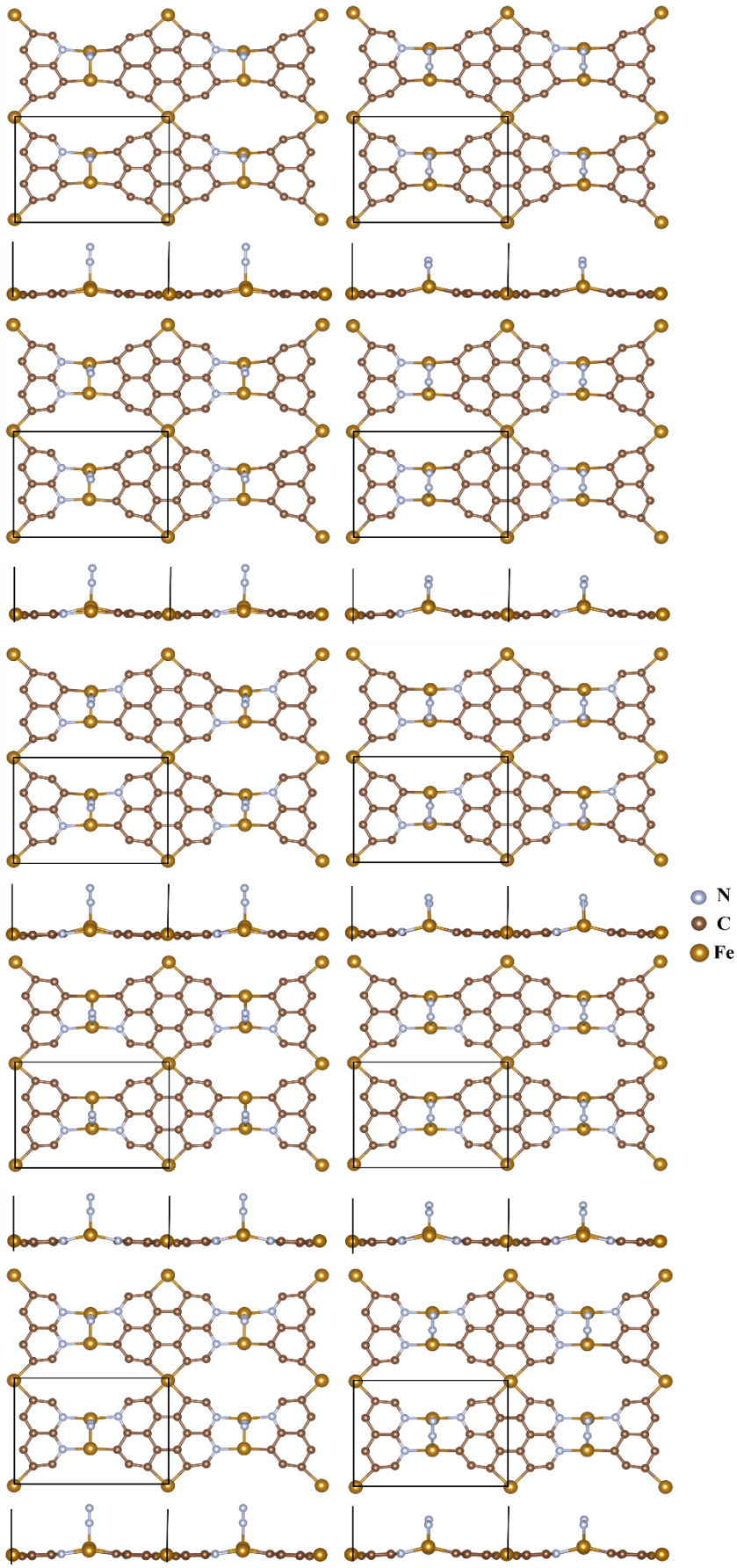

Supplementary Figure 7. Different adsorption structures of N_2 adsorption on $Fe_3@N_xC_{20-x}$ (x = 1~3), with the unit cells marked by black lines.

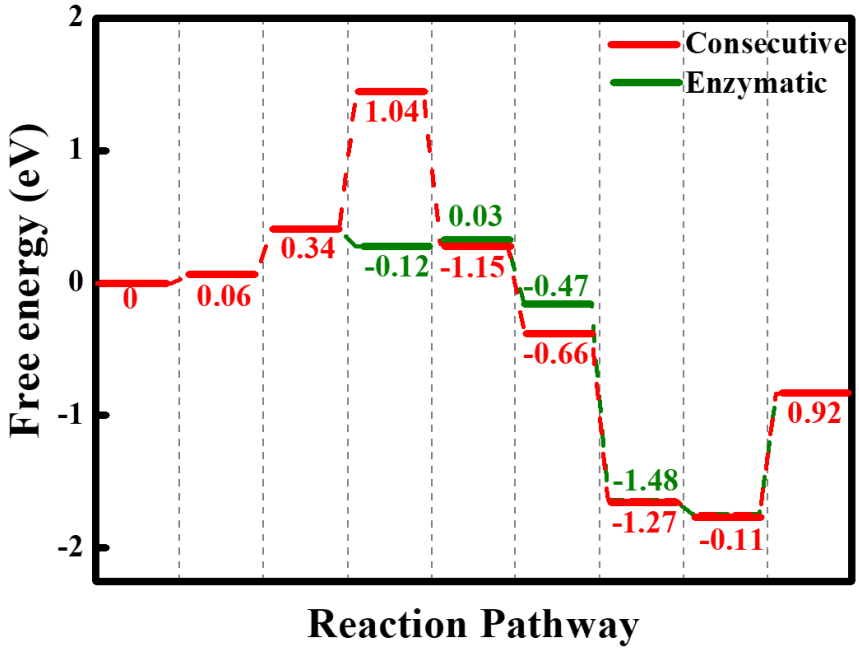

Supplementary Figure 8. The free energy diagram of eNRR through consecutive/ enzymatic (in red/green) pathway on $Fe_3@N_4C_{16}$ including the solvation effect. Data denote the ΔG of each elementary step.

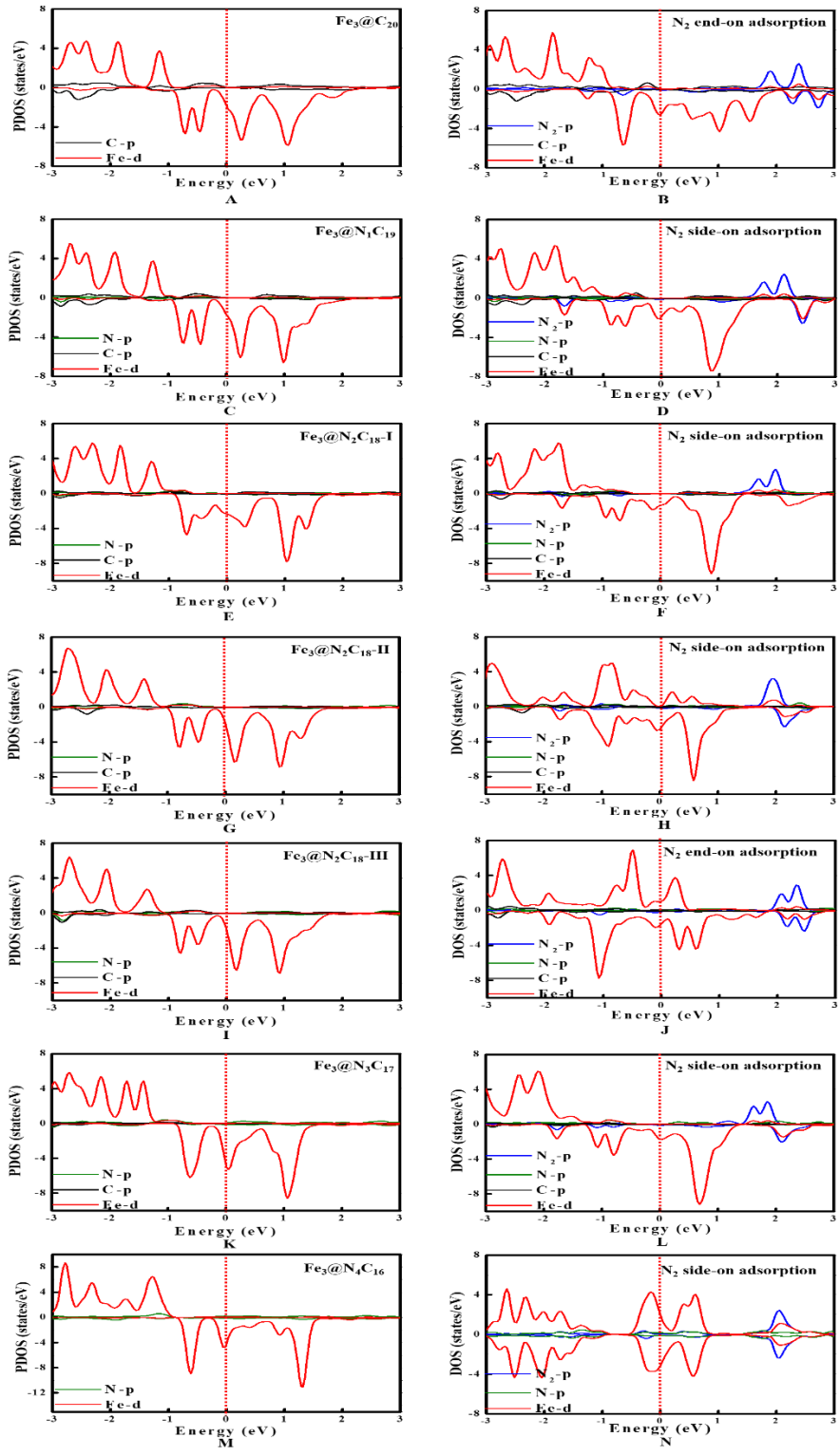

Supplementary Figure 9. The PDOS of $Fe_3@N_xC_{20-x}$ (x = 0~4) structures without and with N_2 adsorption for $Fe_3@C_{20}$ (A,B) $Fe_3@N_1C_{19}$ (C,D), $Fe_3@N_2C_{18}$-I (E,F), $Fe_3@N_2C_{18}$-II (G,H), $Fe_3@N_2C_{18}$-III (I,J), $Fe_3@N_3C_{17}$ (K,L), and $Fe_3@N_4C_{16}$ (M,N). Only the *d*-orbital of the Fe_2 site and its 4 bonded C/N atoms are considered in the figure. The black, red, green and blue solid lines represent the C-*p*, Fe-*d*, doped N-*p* and $*N_2$ molecular *p* orbitals, respectively, and the red dashed line indicates the Fermi energy level.